ISSN 2186-6570

Classical Capacity of Turbulent Channels in *M*-ary Phase Shift Keying Signal Format

Kentaro Kato

Quantum Communication Research Center,
Quantum ICT Research Institute, Tamagawa University
6-1-1 Tamagawa-gakuen, Machida, Tokyo 194-8610 Japan

Tamagawa University Quantum ICT Research Institute Bulletin, Vol.13, No.1, 27-34, 2023

Tamagawa University Quantum ICT Research Institute Bulletin
Vol.13 No.1 : 27–34 (2023)

Classical Capacity of Turbulent Channels in M-ary Phase Shift Keying Signal Format

Kentaro Kato
Quantum Communication Research Center,
Quantum ICT Research Institute, Tamagawa University
6-1-1 Tamagawa-gakuen, Machida, Tokyo 194-8610 Japan
E-mail: kkatop@lab.tamagawa.ac.jp

***Abstract*—Based on a turbulence model described in the literature by Semenov and Vogel [1], we analyzed the classical capacity of turbulent channels for quantum communication systems with M-ary phase shift keying (PSK) coherent state signal and computed the classical capacity of the turbulent channel for $M = 2, 4, 8$ and 16.**

I. Introduction

Quantum communication theory is one of the fundamental theories of quantum information science and plays an essential role in exploring the future possibilities of optical communication systems. If we trace the origin of quantum communication theory to the pioneering work on quantum detection theory by Helstrom, Holevo, Yuen, and others beginning in the late 1960s ([2], [3]), one of the topics that remain unresolved, even though discussions began in the early days of quantum communication theory, is the application of quantum communication theory to free-space optical (FSO) communication applications. In particular, the performance analysis of quantum communication systems using turbulent communication channels and the discussion toward its realization are very challenging issues.

In this article, we explore this challenge using a simple turbulence model described in Ref. [1]. We focus on how well quantum communication systems works in a turbulent atmosphere using an M-ary PSK signal format. The purpose of this study is to seek the possibility of quantum communication systems in a turbulent atmosphere. As the first step, we will use the classical information capacity for quantum communication systems established in the Holevo-Schumacher-Westmoreland theorem to evaluate the performance.

II. Turbulent channels

This article concerns the classical capacity of turbulent channels used in a M-ary PSK signal format with coherent state light. To begin with, we summarize a turbulence model presented in Ref. [1] in this section.

Let us denote the transmission coefficient for optical signals in a turbulent atmosphere by T and the corresponding transmittance by $\eta = |T|^2$ $(0 < \eta \leq 1)$. The transmission coefficient T can be expressed in the form

$$T = t\,\exp(\jmath\varphi) = t\,\cos\varphi + \jmath\, t\,\sin\varphi,$$

where $t = |T|$ $(0 < t \leq 1)$, $\varphi = \arg T$ $(-\pi < \varphi \leq \pi)$, and $\jmath = \sqrt{-1}$.

Let us denote the P-function of a quantum state corresponding to channel input light by $\mathsf{P}_{\rm in}(\alpha)$. Suppose the communication channel only acts as an attenuation process with a fixed transmission coefficient T. Then, the P-function of the output state is expressed as follows [1]:

$$\mathsf{P}_T(\alpha) = \frac{1}{|T|^2}\mathsf{P}_{\rm in}\left(\frac{\alpha}{T}\right).$$

The P-function of the coherent state $|\beta_0\rangle_{\rm coh}$ of complex amplitude β_0 is $\mathsf{P}(\alpha) = \delta(\alpha - \beta_0)$ [4]. When coherent light $|\beta_0\rangle_{\rm coh}$ is passing through the attenuation channel with a fixed transmission coefficient T, the quantum state of the output light is given by

$$\begin{aligned}\hat{\rho}_T &= \int \mathsf{P}_T(\alpha)|\alpha\rangle_{\rm coh}\langle\alpha|\,{\rm d}^2\alpha\Big|_{\mathsf{P}_{\rm in}(\alpha)=\delta(\alpha-\beta_0)} \\ &= |T\beta_0\rangle_{\rm coh}\langle T\beta_0|. \qquad (1)\end{aligned}$$

Namely, the input coherent state $|\beta_0\rangle_{\rm coh}$ changes to a coherent state $|T\beta_0\rangle_{\rm coh}$ after passing through a stable attenuation channel.

In the case of a turbulent atmosphere, the transmission coefficient T varies stochastically. To describe such a probabilistic nature of a turbulent atmosphere, one can use a probability distribution $\mathcal{P}(T)$ of T, which is called the probability distribution of transmission coefficient (PDTC) [1]. Then, the P-function of the quantum state after passing through a turbulent chanel that is characterized by $\mathcal{P}(T)$ is given by

$$\begin{aligned}\mathsf{P}_{\rm out}(\alpha) &= \int_{|T|^2\leq 1}\mathcal{P}(T)\mathsf{P}_T(\alpha){\rm d}^2T \\ &= \int_{|T|^2\leq 1}\mathcal{P}(T)\frac{1}{|T|^2}\mathsf{P}_{\rm in}\left(\frac{\alpha}{T}\right){\rm d}^2T,\end{aligned}$$

where ${\rm d}^2T \equiv {\rm d}t{\rm d}\varphi$.

Based on the formula above, the output state for the coherent state input $|\beta_0\rangle_{\rm coh}$ is expressed as

$$\begin{aligned}\hat{\rho}_{\rm out}(\beta_0) &= \int \mathsf{P}_{\rm out}(\alpha)|\alpha\rangle_{\rm coh}\langle\alpha|{\rm d}^2\alpha\Big|_{\mathsf{P}_{\rm in}(\alpha)=\delta(\alpha-\beta_0)} \\ &= \int_{|T|^2\leq 1}\mathcal{P}(T)|T\beta_0\rangle_{\rm coh}\langle T\beta_0|{\rm d}^2T, \qquad (2)\end{aligned}$$

which is the statistical mixture of coherent states $|T\beta_0\rangle_{\rm coh}$ with a PDTC $\mathcal{P}(T)$.

Suppose a situation where a turbulent atmosphere consists of many small eddies. Let T_k be a random variable associated with the transmission coefficient of a small eddy. Then, the total effect is obtained by $T = \prod_k T_k$. Letting $T_k = t_k \exp(\jmath\varphi_k) = \exp(\ln t_k)\exp(\jmath\varphi_k)$, the overall transmission coefficient is given by

$$T = \exp\left(\sum_k \ln t_k\right)\exp\left(\jmath\sum_k \varphi_k\right).$$

By applying the central limit theorem to random variables $\ln t$ and φ with the assumption that these random variables are correlated with a correlation coefficient s, one can obtain a probability density function $f(\ln t, \varphi)$ such that t is lognormal (that is, $\ln t$ is normally distributed) and φ is normal. By changing the random variable $\ln t$ to t in $f(\ln t, \varphi)$, we obtaine [1]

$$\begin{aligned}\mathcal{P}(t,\varphi) \approx\ & \frac{1}{2\pi t\sigma_\theta\sigma_\varphi\sqrt{1-s^2}} \\ & \times\exp\Big(-\frac{1}{2(1-s^2)} \\ & \times\Big[\left(\frac{\ln t+\bar\theta}{\sigma_\theta}\right)^2+\left(\frac{\varphi}{\sigma_\varphi}\right)^2 \\ & +2s\left(\frac{\ln t+\bar\theta}{\sigma_\theta}\right)\left(\frac{\varphi}{\sigma_\varphi}\right)\Big]\Big), \quad (3)\end{aligned}$$

where $\bar\theta$ and σ_θ are the expectation and the standard deviation of the random variable $-\ln t$, respectively, and σ_φ is the standard deviation of the random variable φ, and where the expectation of the random variable φ is assumed to be zero, and $\sigma_\theta \ll \bar\theta$, $\sigma_\varphi \ll \pi$. A concrete example of $\mathcal{P}(t,\varphi)$ is shown in Fig. 1.

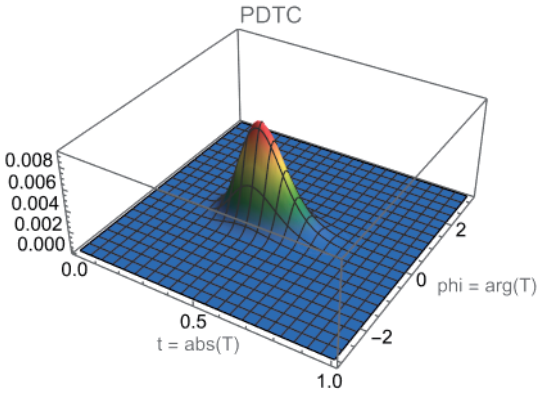

Fig. 1. (Example) $\mathcal{P}(t,\varphi)$ vs. t-φ. $\bar\theta = 0.8$, $\sigma_\theta = 0.2$, and $\sigma_\varphi = 0.3$, $s = 0.0$.

The above derivation process of PDTCs allows t and φ to exceed their normal ranges. That is, the integral of the right-hand side of Eq. (3) over the ranges $(0, 1]$ for t and $(-\pi, \pi]$ for φ may not be one. Therefore, when Eq.(3) is used in actual computer calculations, appropriate normalization is performed in advance. In addition, the discretization of $\mathcal{P}(t,\varphi)$ is also performed for computation. A concrete procedure of normalization and discretization has been presented in Ref. [5].

III. Classical Capacity of Turbulent Channels

According to the Holevo-Schumacher-Westmoreland theorem [6], [7], [8], the capacity of a discrete classical-quantum channel $m \mapsto \hat\rho'_m$ with the input alphabet $\mathcal{A} = \{1, 2, \ldots, M\}$ and the output alphabet $\mathcal{B} = \{\hat\rho'_1, \hat\rho'_2, \ldots, \hat\rho'_M : \hat\rho'_m \geq 0, {\rm tr}\hat\rho'_m = 1\}$ is given by

$$C = \max_\xi \Big[H(\sum_{m=1}^M \xi_m\hat\rho'_m) - \sum_{m=1}^M \xi_m H(\hat\rho'_m)\Big], \quad (4)$$

where $H(\hat\rho') = -{\rm tr}\hat\rho'\log_2\hat\rho'$ is the von Neumann entropy of $\hat\rho'$ and $\xi = (\xi_1, \xi_2, \ldots, \xi_M)$ is a distribution of the letters ($\xi_m \geq 0$, $\sum_m \xi_m = 1$) .

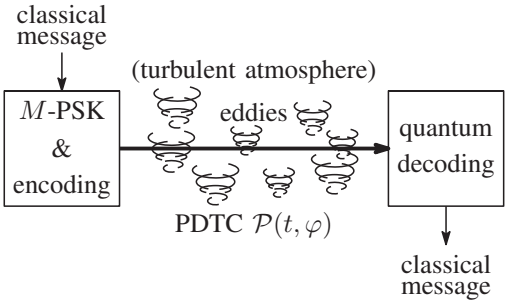

Fig. 2. Communication Model

Suppose turbulent channels are used in the M-ary PSK signal format (Fig. 2). The signal set of M-ary PSK coherent state signal is given by

$$\mathcal{S} = \Big\{\hat\rho_m = |\alpha_m\rangle_{\rm coh}\langle\alpha_m| : m = 1, 2, \ldots, M\Big\}, \quad (5)$$

where the mth complex amplitude of the coherent state signal is defined as

$$\alpha_m = \alpha\exp[\jmath\frac{2\pi}{M}(m-1)], \qquad \alpha > 0. \quad (6)$$

Each PSK coherent state signal $\hat\rho_m$ is transmitted via a turbulent channel with $\mathcal{P}(T)$. The output state is $\hat\rho'_m = \hat\rho_{\rm out}(\alpha_m)$. Since the PSK signals in $\mathcal{S}$ are symmetric, in the sense of $\hat\rho_m = \hat U^{\dagger m-1}\hat\rho_1\hat U^{m-1}$ by a unitary operator $\hat U$, and the PDTC $\mathcal{P}(T)$ is independent of any signal parameters of $\mathcal{S}$, the received signal states $\hat\rho'_m$ are also symmetric. Applying the result in [9] to these symmetric signal states, the uniform distribution, $\xi = (1/M, 1/M, \ldots, 1/M)$, is optimal for achieving the classical capacity. Therefore, the classical capacity of the turbulent channel $m \mapsto \hat\rho'_m$ is given by

$$C = H(\hat\rho') - H(\hat\rho'_1), \quad (7)$$

where

$$\hat{\rho}' = \frac{1}{M}\sum_{m=1}^{M}\hat{\rho}'_m. \tag{8}$$

Here let us consider a non-turbulent case for reference. Suppose the communication channel only acts as an attenuation process from $|\beta_0\rangle_{\rm coh}$ to $|T\beta_0\rangle_{\rm coh}$ with a stable T. Then, the classical capacity of the channel $m \mapsto |T\beta_0\rangle_{\rm coh}$ is given by [9]

$$C = -\sum_{k=1}^{M}\lambda'_k \log_2 \lambda'_k, \tag{9}$$

where

$$\lambda'_k = \frac{1}{M}\sum_{\ell=1}^{M} A'_{(1,\ell)}\cos\Big[\Theta'_{(1,\ell)} - \frac{2\pi}{M}k(\ell-1)\Big]; \tag{10}$$

$$A'_{(k,\ell)} = \exp\Big[-2|T\alpha|^2\sin^2\Big[\frac{\pi}{M}(\ell-k)\Big]\Big]; \tag{11}$$

$$\Theta'_{(k,\ell)} = |T\alpha|^2\sin\Big[\frac{2\pi}{M}(\ell-k)\Big]. \tag{12}$$

To investigate the performance of quantum communication systems using the PSK signal format, we calculated the channel capacity and displayed the results in figures 3 to 12. Figs. 3 and 4 represent the cases when $M = 2$, Figs. 5 and 6 for $M = 4$, Figs. 7 and 8 for $M = 8$, Figs. 9 and 10 for $M = 16$, and Figs. 11 and 12 combine all the cases.

In each figure, we used several parameters, such as $\bar{\theta}$ (the expectation value of $-\ln t$), σ_θ (the standard deviation of $-\ln t$: a measure of channel classical noise in amplitude direction), and σ_φ (the standard deviation of φ;a measure of channel classical noise in phase direction). For reference, we included a non-turbulent case calculated from Eq.(7) with the condition $T = t\exp[\jmath\cdot 0] = t$ (shown as black dotted lines). In the small grids of each figure, the top-left represents the least noisy cases, while the bottom-right shows the most noisy ones. The vertical axis shows the classical capacity in bits per transmitted signal, and the horizontal axis represents the average number of received signal photons ($\bar{n}_{\rm rx} = {\rm tr}\hat{\rho}'\hat{n}$, where $\hat{n}$ is the number operator).

For $M = 2$ and 4, the maximum capacities ($C = 1$ or 2) can be achieved by increasing the signal power in our setup, as shown in Figs. 3 to 6 and parts of Figs. 11 and 12. However, for $M = 8$ and 16, we observed cases where the maximum capacity ($C = 3$ or 4) could not be achieved, especially when σ_φ (phase noise) was 0.2 and 0.3. This phenomenon may be explained by the phase fluctuation margins between signals in 8-PSK and 16-PSK signal formats. Roughly speaking, these margins are $(2\pi/8)/2 \sim 0.4$ for $M = 8$ and $(2\pi/16)/2 \sim 0.2$ for $M = 16$. Compared to these margins, $\sigma_\varphi = 0.2$ and 0.3 represent significant phase fluctuations, leading to nonachievability to the maximum capacities in those cases.

As menthioned above, we observed the degradation effect for communication performance due to classical noise in a turbulent atmosphere for $M = 8$ and 16. What is the critical amount of classical noise for each PSK signal format? The determination of the critical amount of classical noise for each PSK signal format is a subject for future research.

In our computation, we used $\bar{\theta} = 0.8, 1.0, 1.2$, $\sigma_\theta = 0.1, 0.2, 0.3$, $\sigma_\varphi = 0.1, 0.2, 0.3$, and $s = 0.0$. It is unclear whether the values used in this study are realistic and appropriate. Therefore, cooperation with experimental researchers is essential to find a realistic and reasonable setting.

IV. Summary

The classical capacity of turbulent channels using coherent state signals in the phase shift keying (PSK) format was investigated. Based on the turbulence model of Ref. [1], the classical capacity for M-ary PSK coherent state signal in a turbulent atmosphere was analyzed and computed for $M = 2, 4, 8$, and 16. We observed the degradation effect for communication performance due to classical noise in a turbulent atmosphere for $M = 8$ and 16. We pointed out that determining the critical amount of classical noise, which significantly degrades communication performance, and the consistency of the modeling parameters with real-world situations remains for future study. These will be discussed elsewhere.

Acknowledgments

This material is based upon work supported by the Air Force Office of Scientific Research under award number FA2386-22-1-4030.

References

[1] A.A. Semenov and W. Vogel, "Quantum light in the turbulent atmosphere," Phys. Rev. A, vol. 80, iss. 2, 021802(R), Aug. 2009.
[2] C.W. Helstrom, Quantum Detection and Estimation Theory (Academic, New York, 1976).
[3] A.S. Holevo, Probabilistic and Statistical Aspects of Quantum Theory (NorthHolland, Amsterdam, 1982).
[4] D.F. Walls and G.J. Milburn, Quantum Optics (Springer, Berlin, 1994).
[5] K. Kato, "A study on quantum communication through turbulent atmosphere," The 45th Symposium. Information Theory and its Applications (SITA2022), Noboribetsu, Hokkaido, Japan, Nov. 29 - Dec. 2, 2022 (in japanese).
[6] B. Schumacher and M.D. Westmoreland, "Sending classical information via noisy quantum channels," Phys. Rev. A, vol. 56, no. 1, pp. 131 - 138, Jul. 1997.
[7] A.S. Holevo, "The capacity of the quantum channel with general signal states," IEEE Trans. Inf. Theory, vol. 44, no. 1, pp. 269 - 273, Jan. 1998; arXiv:quant-ph/9611023.
[8] A.S. Holevo, "Coding theorems for quantum channels," Tamagawa University Research Review, no. 4, pp. 1 - 33, 1998; arXiv:quant-ph/9809023.
[9] K. Kato, M. Osaki, and O. Hirota, "Derivation of classical capacity of a quantum channel for a discrete information source," Phys. Lett. A, vol. 251, iss. 3, pp. 157 - 163, Jan. 1999.

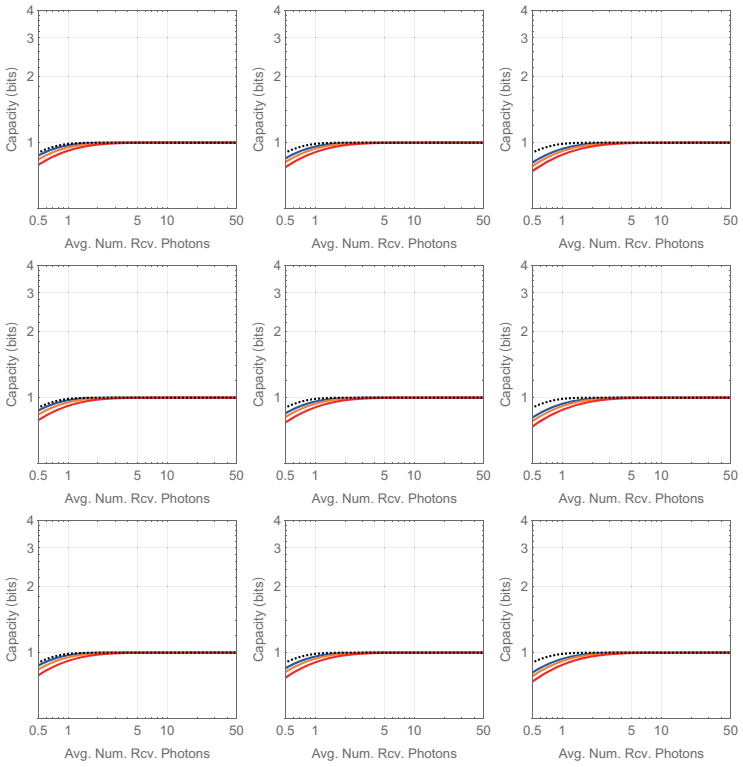

Fig. 3. Classical Capacity C vs. Average Number of Received Signal Photons $\bar{n}_{\mathrm{rx}}$ for Fixed σ_φ at $M = 2$ (Case A, $M = 2$). Left column: $\sigma_\varphi = 0.1$; Center column: $\sigma_\varphi = 0.2$; Right column: $\sigma_\varphi = 0.3$. Top row: $\bar{\theta} = 0.8$; Middle row: $\bar{\theta} = 1.0$; Bottom row: $\bar{\theta} = 1.2$. Blue: $\sigma_\theta = 0.1$; Orange: $\sigma_\theta = 0.2$; Red: $\sigma_\theta = 0.3$; Black dotted: non-turbulent (reference).

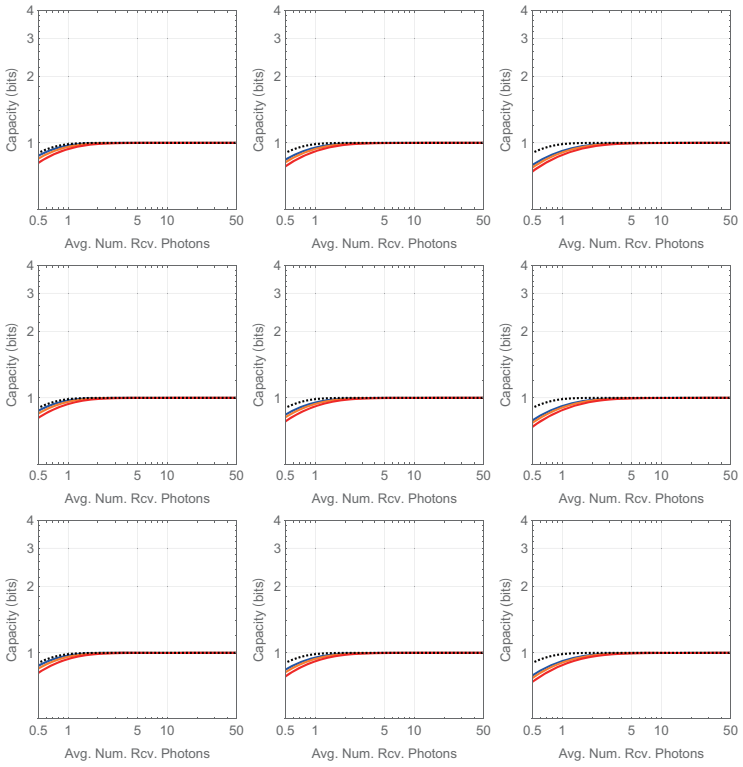

Fig. 4. Classical Capacity C vs. Average Number of Received Signal Photons $\bar{n}_{\mathrm{rx}}$ for Fixed σ_θ at $M = 2$ (Case B, $M = 2$). Left column: $\sigma_\theta = 0.1$; Center column: $\sigma_\theta = 0.2$; Right column: $\sigma_\theta = 0.3$. Top row: $\bar{\theta} = 0.8$; Middle row: $\bar{\theta} = 1.0$; Bottom row: $\bar{\theta} = 1.2$. Blue: $\sigma_\varphi = 0.1$; Orange: $\sigma_\varphi = 0.2$; Red: $\sigma_\varphi = 0.3$; Black dotted: non-turbulent (reference).

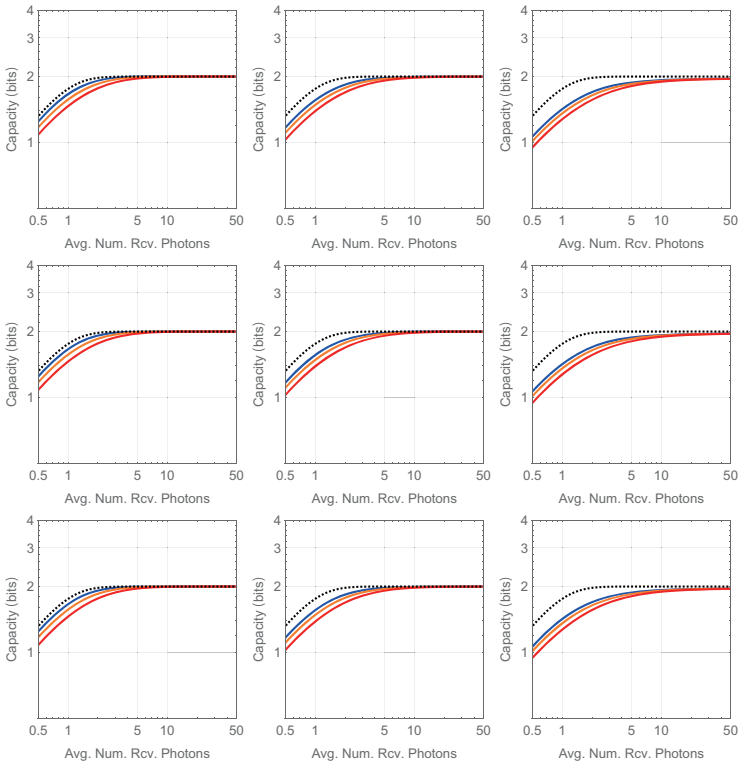

Fig. 5. Classical Capacity C vs. Average Number of Received Signal Photons $\bar{n}_{\mathrm{rx}}$ for Fixed σ_φ at $M = 4$ (Case A, $M = 4$). Left column: $\sigma_\varphi = 0.1$; Center column: $\sigma_\varphi = 0.2$; Right column: $\sigma_\varphi = 0.3$. Top row: $\bar{\theta} = 0.8$; Middle row: $\bar{\theta} = 1.0$; Bottom row: $\bar{\theta} = 1.2$. Blue: $\sigma_\theta = 0.1$; Orange: $\sigma_\theta = 0.2$; Red: $\sigma_\theta = 0.3$; Black dotted: non-turbulent (reference).

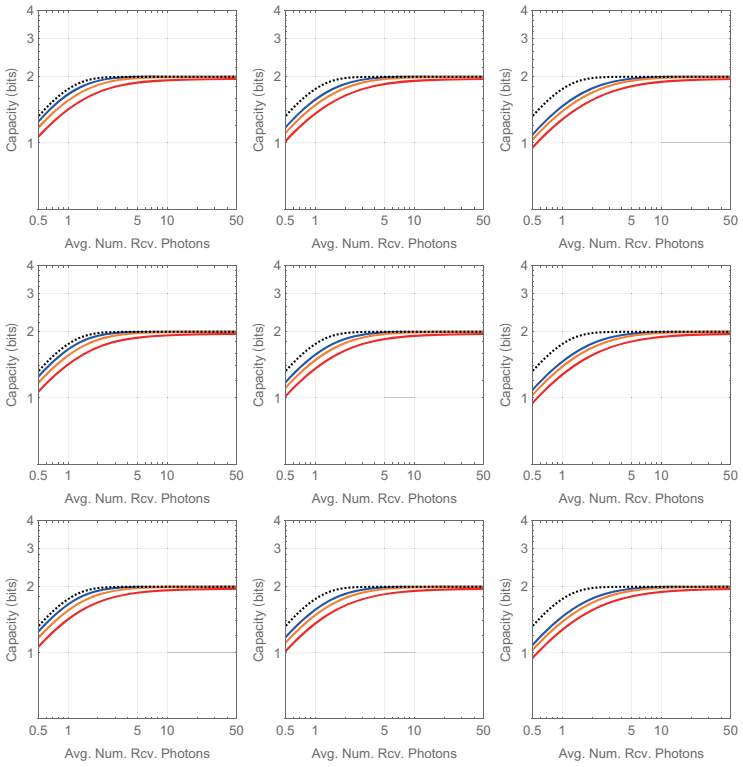

Fig. 6. Classical Capacity C vs. Average Number of Received Signal Photons $\bar{n}_{\mathrm{rx}}$ for Fixed σ_θ at $M = 4$ (Case B, $M = 4$). Left column: $\sigma_\theta = 0.1$; Center column: $\sigma_\theta = 0.2$; Right column: $\sigma_\theta = 0.3$. Top row: $\bar{\theta} = 0.8$; Middle row: $\bar{\theta} = 1.0$; Bottom row: $\bar{\theta} = 1.2$. Blue: $\sigma_\varphi = 0.1$; Orange: $\sigma_\varphi = 0.2$; Red: $\sigma_\varphi = 0.3$; Black dotted: non-turbulent (reference).

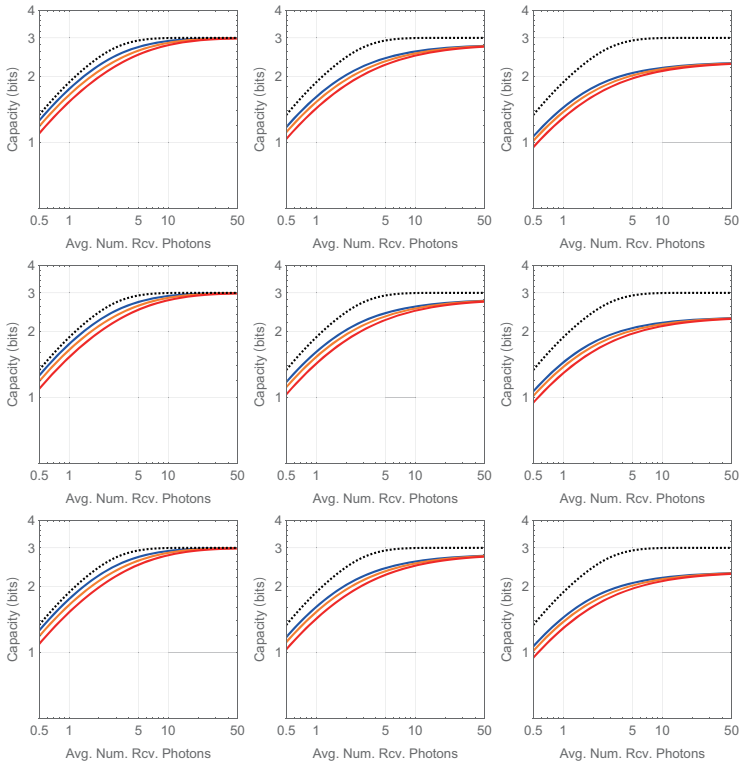

Fig. 7. Classical Capacity C vs. Average Number of Received Signal Photons $\bar{n}_{\mathrm{rx}}$ for Fixed σ_φ at $M = 8$ (Case A, $M = 8$). Left column: $\sigma_\varphi = 0.1$; Center column: $\sigma_\varphi = 0.2$; Right column: $\sigma_\varphi = 0.3$. Top row: $\bar{\theta} = 0.8$; Middle row: $\bar{\theta} = 1.0$; Bottom row: $\bar{\theta} = 1.2$. Blue: $\sigma_\theta = 0.1$; Orange: $\sigma_\theta = 0.2$; Red: $\sigma_\theta = 0.3$; Black dotted: non-turbulent (reference).

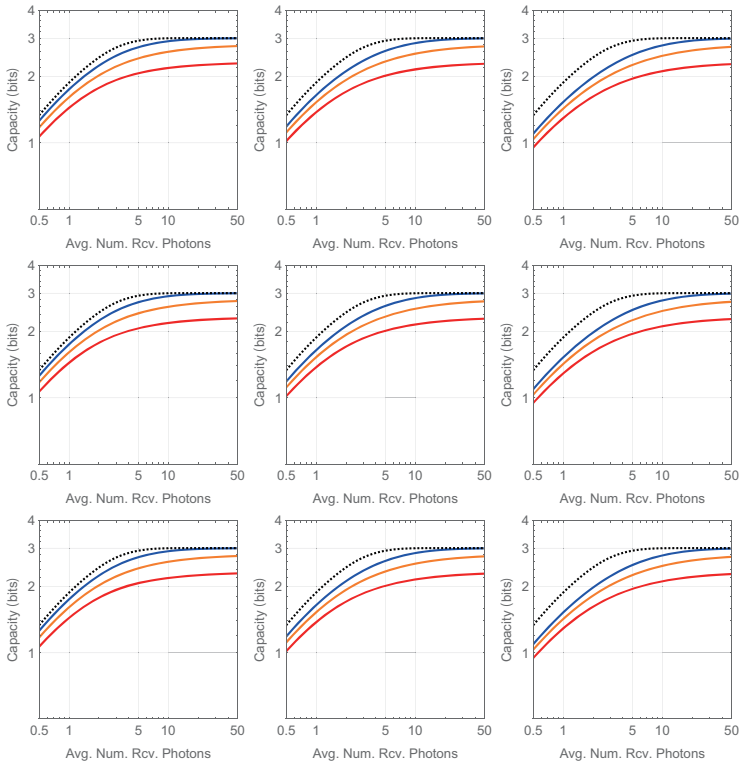

Fig. 8. Classical Capacity C vs. Average Number of Received Signal Photons $\bar{n}_{\mathrm{rx}}$ for Fixed σ_θ at $M = 8$ (Case B, $M = 8$). Left column: $\sigma_\theta = 0.1$; Center column: $\sigma_\theta = 0.2$; Right column: $\sigma_\theta = 0.3$. Top row: $\bar{\theta} = 0.8$; Middle row: $\bar{\theta} = 1.0$; Bottom row: $\bar{\theta} = 1.2$. Blue: $\sigma_\varphi = 0.1$; Orange: $\sigma_\varphi = 0.2$; Red: $\sigma_\varphi = 0.3$; Black dotted: non-turbulent (reference).

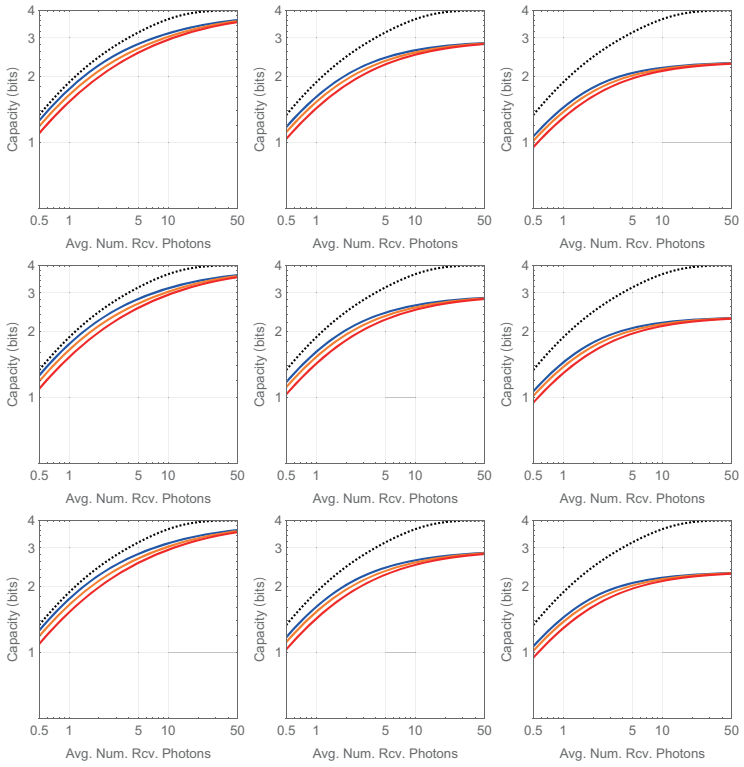

Fig. 9. Classical Capacity C vs. Average Number of Received Signal Photons $\bar{n}_{\mathrm{rx}}$ for Fixed σ_φ at $M = 16$ (Case A, $M = 16$). Left column: $\sigma_\varphi = 0.1$; Center column: $\sigma_\varphi = 0.2$; Right column: $\sigma_\varphi = 0.3$. Top row: $\bar{\theta} = 0.8$; Middle row: $\bar{\theta} = 1.0$; Bottom row: $\bar{\theta} = 1.2$. Blue: $\sigma_\theta = 0.1$; Orange: $\sigma_\theta = 0.2$; Red: $\sigma_\theta = 0.3$; Black dotted: non-turbulent (reference).

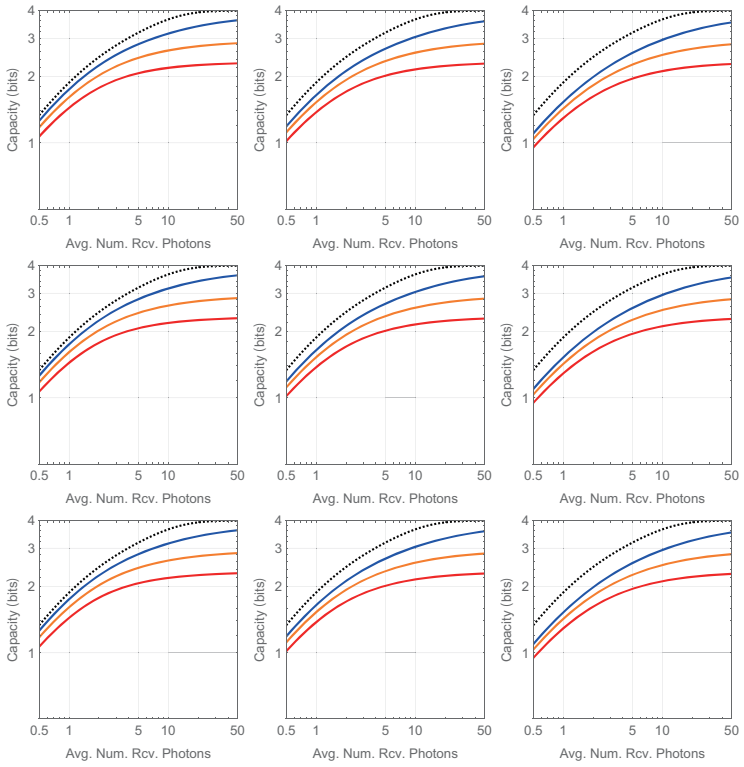

Fig. 10. Classical Capacity C vs. Average Number of Received Signal Photons $\bar{n}_{\mathrm{rx}}$ for Fixed σ_θ at $M = 16$ (Case B, $M = 16$). Left column: $\sigma_\theta = 0.1$; Center column: $\sigma_\theta = 0.2$; Right column: $\sigma_\theta = 0.3$. Top row: $\bar{\theta} = 0.8$; Middle row: $\bar{\theta} = 1.0$; Bottom row: $\bar{\theta} = 1.2$. Blue: $\sigma_\varphi = 0.1$; Orange: $\sigma_\varphi = 0.2$; Red: $\sigma_\varphi = 0.3$; Black dotted: non-turbulent (reference).

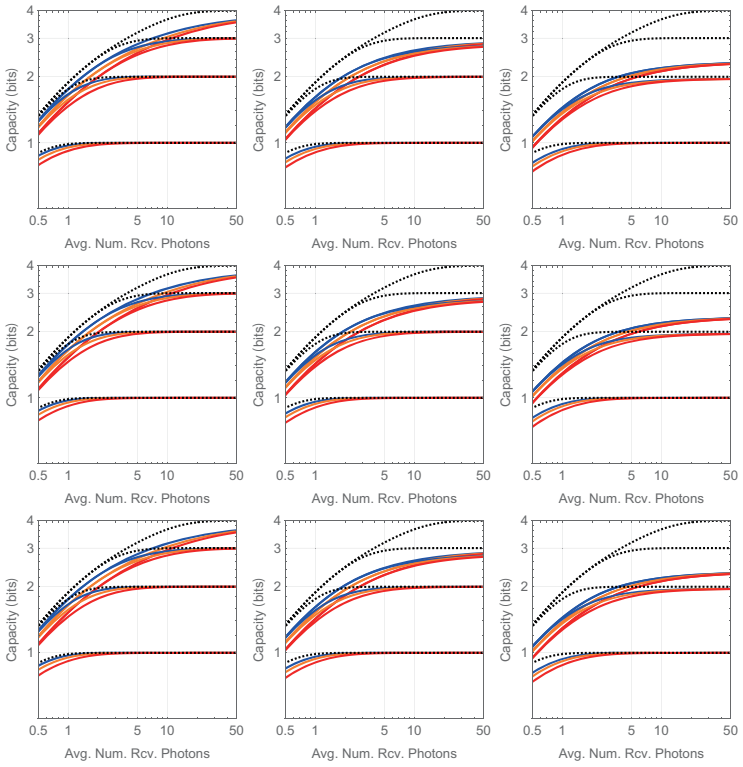

Fig. 11. Classical Capacity C vs. Average Number of Received Signal Photons $\bar{n}_{\mathrm{rx}}$ for Fixed σ_φ (Case A, $M = 2, 4, 8, 16$). Left column: $\sigma_\varphi = 0.1$; Center column: $\sigma_\varphi = 0.2$; Right column: $\sigma_\varphi = 0.3$. Top row: $\bar{\theta} = 0.8$; Middle row: $\bar{\theta} = 1.0$; Bottom row: $\bar{\theta} = 1.2$. Blue: $\sigma_\theta = 0.1$; Orange: $\sigma_\theta = 0.2$; Red: $\sigma_\theta = 0.3$; Black dotted: non-turbulent (reference).

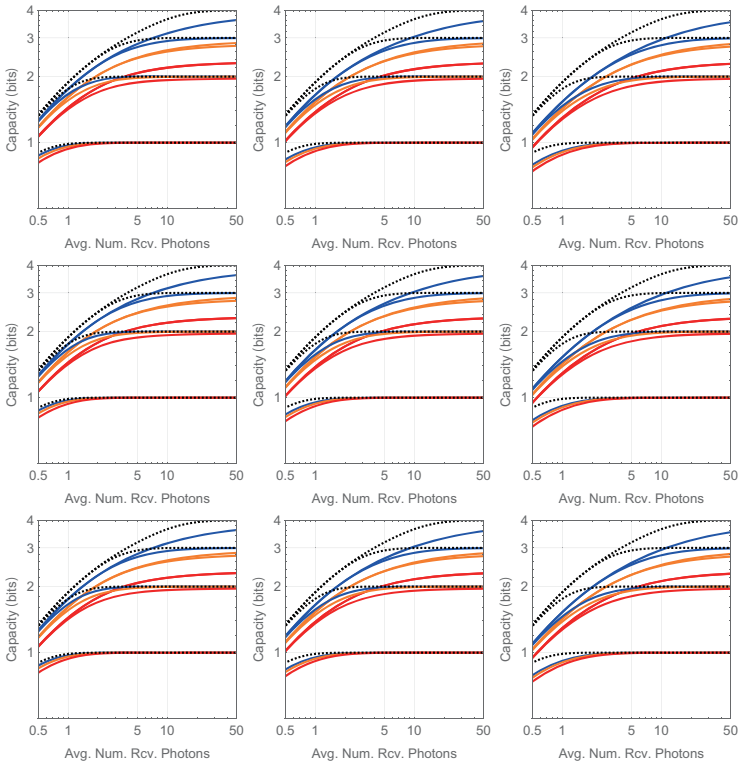

Fig. 12. Classical Capacity C vs. Average Number of Received Signal Photons $\bar{n}_{\mathrm{rx}}$ for Fixed σ_θ (Case B, $M = 2, 4, 8, 16$). Left column: $\sigma_\theta = 0.1$; Center column: $\sigma_\theta = 0.2$; Right column: $\sigma_\theta = 0.3$. Top row: $\bar{\theta} = 0.8$; Middle row: $\bar{\theta} = 1.0$; Bottom row: $\bar{\theta} = 1.2$. Blue: $\sigma_\varphi = 0.1$; Orange: $\sigma_\varphi = 0.2$; Red: $\sigma_\varphi = 0.3$; Black dotted: non-turbulent (reference).